International Journal of Thermophysics, Vol. 3, No. 1, 1982

Measurement of the Enthalpy and Specific Heat of a Be_2C–Graphite–UC_2 Reactor Fuel Material to 1980 K

E. P. Roth[1]

Received October 26, 1981

The enthalpy and specific heat of a Be_2C–Graphite–UC_2 composite nuclear fuel material have been measured over the temperature range 298–1980 K using both differential scanning calorimetry and liquid argon vaporization calorimetry. The fuel material measured was developed at Sandia National Laboratories for use in pulsed test reactors. The material is a hot-pressed composite consisting of 40 vol% Be_2C, 49.5 vol% graphite, 3.5 vol% UC_2, and 7.0 vol% void. The specific heat was measured with the differential scanning calorimeter over the temperature range 298–950 K, while the enthalpy was measured over the range 1185–1980 K with the liquid argon vaporization calorimeter. The normal spectral emittance at a wavelength of 6.5×10^{-5} cm was also measured over the experimental temperature range. The combined experimental enthalpy data were fit using a spline routine and differentiated to give the specific heat. Comparison of the measured specific heat of the composite to the specific heat calculated by summing the contributions of the individual components indicates that the specific heat of the Be_2C component differs significantly from literature values and is approximately 0.56 $cal \cdot g^{-1} \cdot K^{-1}$ ($2.3 \times 10^3 J \cdot kg^{-1} \cdot K^{-1}$) for temperatures above 1000 K.

KEY WORDS: Reactor fuel; liquid argon calorimeter; vaporization calorimeter; enthalpy; specific heat; Be_2C–Graphite–UC_2.

1. INTRODUCTION

Several composite nuclear fuel materials have been developed for pulsed reactors at Sandia National Laboratories [1–4]. The most recently developed composite, Be_2C–Graphite–UC_2, is designed to have better high temperature performance than any of the previous fuels. This fuel is designed to operate in a pulsed reactor environment where high flux neutron pulses result in significant thermal stresses. The inclusion of Be_2C

[1] Sandia National Laboratories, Albuquerque, New Mexico 87185, U.S.A.

0195-928X/82/0300-0045$03.00/0

as part of this fuel material is intended to give the fuel high volumetric enthalpy (to permit higher energy pulses and to reduce the temperature rise during the pulse), while the graphite is designed to increase the thermal stress resistance (and yield a simpler pellet geometry). This fuel should extend the maximum pulse temperature to 2070 K without material degradation.

The volumetric enthalpy and specific heat were originally estimated from published data on the specific heat of the component materials. This calculation should give accurate results, since previous work has indicated that the additivity of heat capacities is valid for similar materials [3]. However, the specific heat of the Be_2C component has only been measured in an impure state at low temperatures ($T < 1470$ K), and significant differences exist in the literature values [5]. Significant variations also exist in the data reported in the literature for graphite [6]. Therefore, the goals of this experimental program were to measure the enthalpy and specific heat of the composite fuel and to obtain a more accurate estimate of the specific heat of the Be_2C component.

2. EXPERIMENTAL

2.1. Calorimeter Systems

A differential scanning calorimeter (model DSC-1, Perkin–Elmer Corp., Norwalk, Conn.) was used to measure the specific heat at low temperatures (298–950 K), while a liquid argon drop calorimeter was used to measure enthalpy at higher temperatures (1185–1980 K). A description of the differential scanning calorimeter is available from the manufacturer.

The liquid argon drop calorimeter system was originally designed as a sensitive instrument for the measurement of high-temperature enthalpy of electrically conductive materials in both the solid and liquid phase [3, 7, 8]. Samples were inductively heated in an inert atmosphere while being electromagnetically levitated without a sample container. However, the electrical conductivity of the Be_2C–Graphite–UC_2 material was too low to allow electromagnetic levitation; therefore, several modifications were required to the original system, and these are described in a later section.

The liquid argon vaporization calorimeter system (Fig. 1) consisted of an rf induction furnace for heating the samples, an inert atmosphere sample chamber, an 800 cm^3 glass dewar filled with liquid argon, gas flow instrumentation, and a minicomputer based digital data acquisition system. The sample was heated in an inert atmosphere sample chamber and then dropped into the dewar of liquid argon. Heat released by the sample while thermally equilibrating with the liquid argon vaporized a portion of the

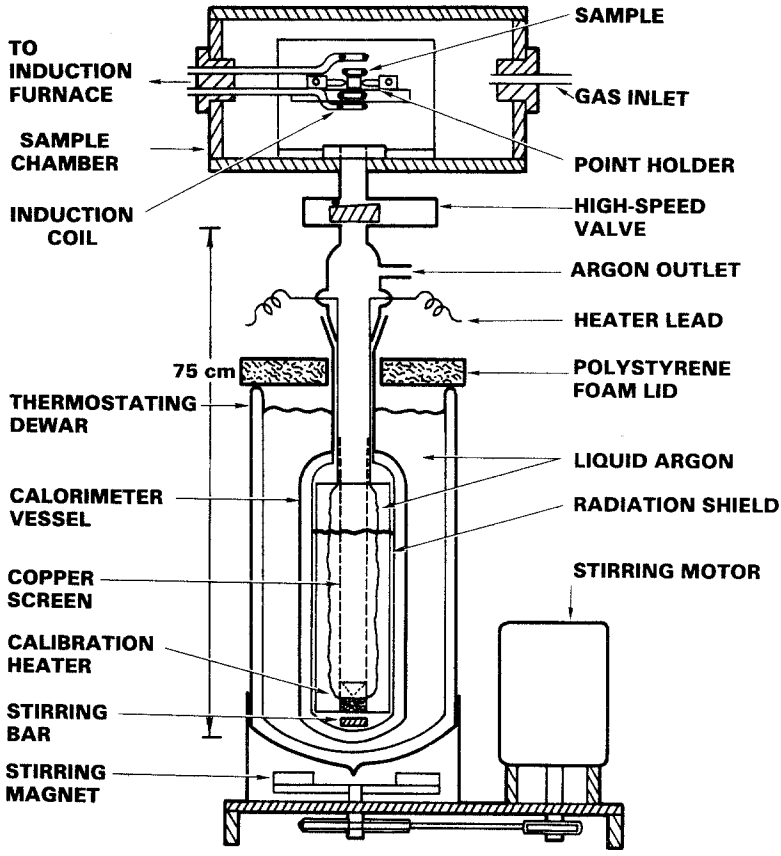

Fig. 1. Liquid argon vaporization calorimeter vessel and sample chamber for heating the samples.

liquid. The resulting gas flow was measured by calibrated flow units and the flow data recorded by the computer. The heat content of the sample was determined from the thermodynamic properties of the liquid argon and the total amount of gas released. Liquid argon was used as the working fluid because of its ready availability, inert properties, high sensitivity factor (ratio of volume change to heat of vaporization), and high "signal-to-noise" ratio for pressure changes [9, 10].

The samples were inductively heated with a 20-kW induction heater (Lepel High Frequency Labs, New York) at a frequency of 450 kHz. Small solenoid-shaped coils (i.d. $\approx$ 1.5 cm) where used to concentrate the rf field. The sample was held inside the coil with a mechanical, point-contact holder using nonreacting (graphite) points. This holding mechanism was solenoid

activated to allow release of the samples at the same moment the induction furnace was turned off. The contact area between the points and the sample was minimized to reduce thermal conduction to the sample and the resultant temperature gradients in the sample. The possibility of error introduced by this holding technique was checked by comparing the enthalpies of graphite, molybdenum, and tantalum measured using both the electromagnetic levitation and the point-holding techniques. The data obtained using the two techniques agreed within a precision of 5%. The sample temperature was controlled manually by varying the power level of the induction heater while the temperature was monitored with an automatic recording pyrometer (Model 8642, Leeds and Northrup). The pyrometer output was recorded both on a strip chart recorder and stored in the computer for later analysis.

Figure 1 shows both the sample chamber and the calorimeter vessel. The sample chamber was connected to the liquid argon dewar through a high-speed, vacuum valve. This valve opened at the same moment that the sample was dropped and was closed by an electronic timer. The gas in the chamber was high purity argon, and the pressure in the sample chamber was regulated so that no significant flow of gas took place between the chamber and the dewar when the valve opened. A constant flow of gas was maintained through the sample chamber during the run to remove any beryllium outgassed from the samples.

The inner dewar containing the liquid argon working fluid was held in a thermostating dewar of liquid argon to reduce heat leaks to the system. The inner dewar contained a copper cup and a black anodized copper mesh screen for guiding and catching the samples. A black anodized metal foil covered the inner wall of the dewar and served as a radiation shield in good thermal contact with the liquid argon. The radiation shields were added after it was observed that at the higher temperatures ($T > 1750$ K), occasionally the samples did not immediately cool but continued to radiate in the rapidly boiling liquid argon, insulated from the liquid by a boundary layer of the vaporized argon for several seconds after initially entering the liquid. A "worst case" measurement of the effect of radiation losses was performed by measuring the enthalpy of a molybdenum sample over the temperature range 1900–2200 K without the presence of the radiation shields. The specific heat determined from the enthalpy data over this temperature range agreed to within 2% of the literature value, indicating that no significant systematic losses were occurring. However, the uncertainty in the measured specific heat was 10% due to scatter in the data. The addition of the radiation shields during the series of measurements of the reactor fuel reduced the scatter in the data by more than a factor of 2, which should result in a corresponding reduction in the uncertainty in the specific heat.

A magnetic stirring bar was placed at the bottom of the inner dewar to reduce thermal stratification in the liquid and to decrease the time to reach thermal equilibrium. The power input due to the stirring action was less than 10^{-4} cal · s^{-1} (4×10^{-4} J · s^{-1}), which resulted in the addition of less than 0.5 cal (2 J) to the system during a typical 60 min run. This power input was held constant throughout the measurement period and resulted in a negligible addition to the background heat input to the system.

An electrical calibration heater was mounted on the copper sample cup at the bottom of the dewar to enable absolute calibration of the entire measuring system. The electrical resistance heater was wound around the copper block, and the electrical resistance was adjusted to approximately 1400 Ω. This resistance value was chosen so that the calibration power input resulted in a pressure rise similar to that observed for the actual samples. Separate leads were used to measure the potential drop across the heater. The current to the heater was determined by measuring the potential drop across a 10 Ω oil-immersed standard resistor placed in series with the heater current line. Power was supplied by a constant current dc power supply for a preset time using an accurate digital electronic timer. The power input to the calorimeter during the calibration period was checked several times and found to be constant within 0.02%. The accuracy of the calibration energy input was 0.05% based upon known instrument accuracies. Figure 2 shows a schematic of the calibration circuitry and the gas flow measurement system.

The gas flow measurement system consisted of a laminar flow unit (50 MJ10 series, Merian Instruments Co., Cleveland, Ohio) and a capacitance-type electronic manometer (Model 170M-7 indicator with a 145AH-10 head, MKS Instruments, Burlington, Mass.) for measuring the pressure drop across the flow unit. The MKS pressure head was calibrated against an accurate dead-weight tester over the pressure range 0–10 Torr, and the observed deviations were fit with a third order polynomial in pressure. The laminar flow unit was also calibrated over the 0–10 Torr pressure range and the flow rate deviations fit as a linear function of pressure.[2] Since the measured flow is a function of temperature, the flow of gas from the calorimeter was first brought to a known reference temperature by passing it through a controlled temperature water bath. After passing through the flow unit, the argon gas was exhausted either into the room or to the outside atmosphere.

The data acquisition system was based upon an HP System 1000 minicomputer (Hewlett-Packard Co., Palo Alto, Calif.). The gas flow rate,

[2]The laminar flow units were calibrated in the Primary Standards Lab, Sandia National Laboratories, using a calibrated volume technique (certificate file no. 3303B). All equipment used was calibrated to NBS traceable standards.

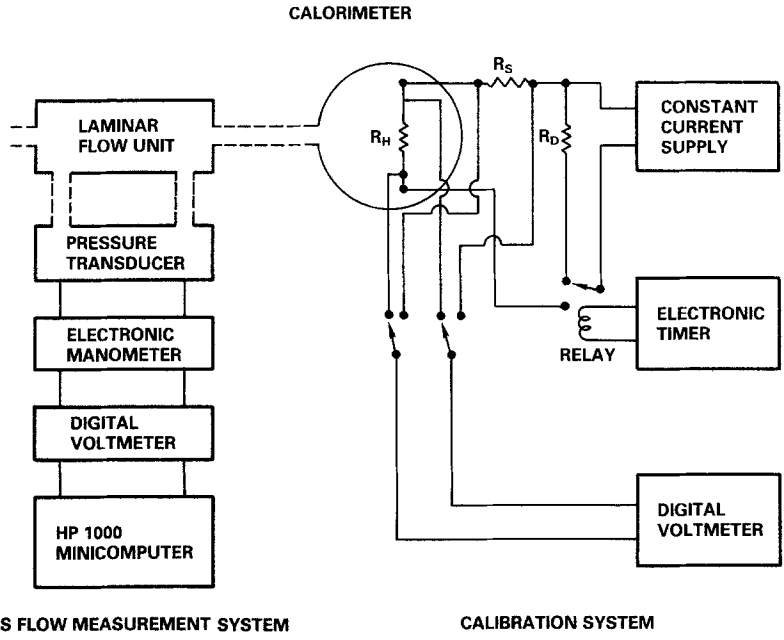

Fig. 2. Schematic of gas flow measurement system and calibration circuit. R_H = calibration heater; R_S = standard resistor for current measurement; R_D = dummy load resistor for initially setting heater power.

background barometric pressure, and the pyrometer output were read by digital voltmeters (DVM) interfaced directly to the computer. The computer recorded the DVM values and the time at which the readings were taken for later analysis.

2.2. Sample Materials

The Be_2C–Graphite–UC_2 fuel material was fabricated by hot pressing a mix containing −325 mesh Be_2C, −325 mesh graphite (grade GL 1008), and −325 mesh UC_2 in a graphite die to 2050°C and 23.8 MPa (3450 psi) pressure. This material was prepared by the Materials Technology Group (CMB-6) of the Los Alamos Scientific Laboratory. The final product contained 40 vol% (39.06 wt%) Be_2C, 49.5 vol% (44.58 wt%) graphite, 3.5 vol% (16.36 wt%) UC_2 (0.371 g U per cm^3, 93% enriched), and 7.0 vol% porosity. The final density was 2.49 $g \cdot cm^{-3}$. The microstructure of the material was characterized by optical microscopy. Figure 3 shows a micrograph of the sample. The UC_2 particle sizes (white areas in figure) were less than 20 μm and were evenly distributed throughout the material. X-

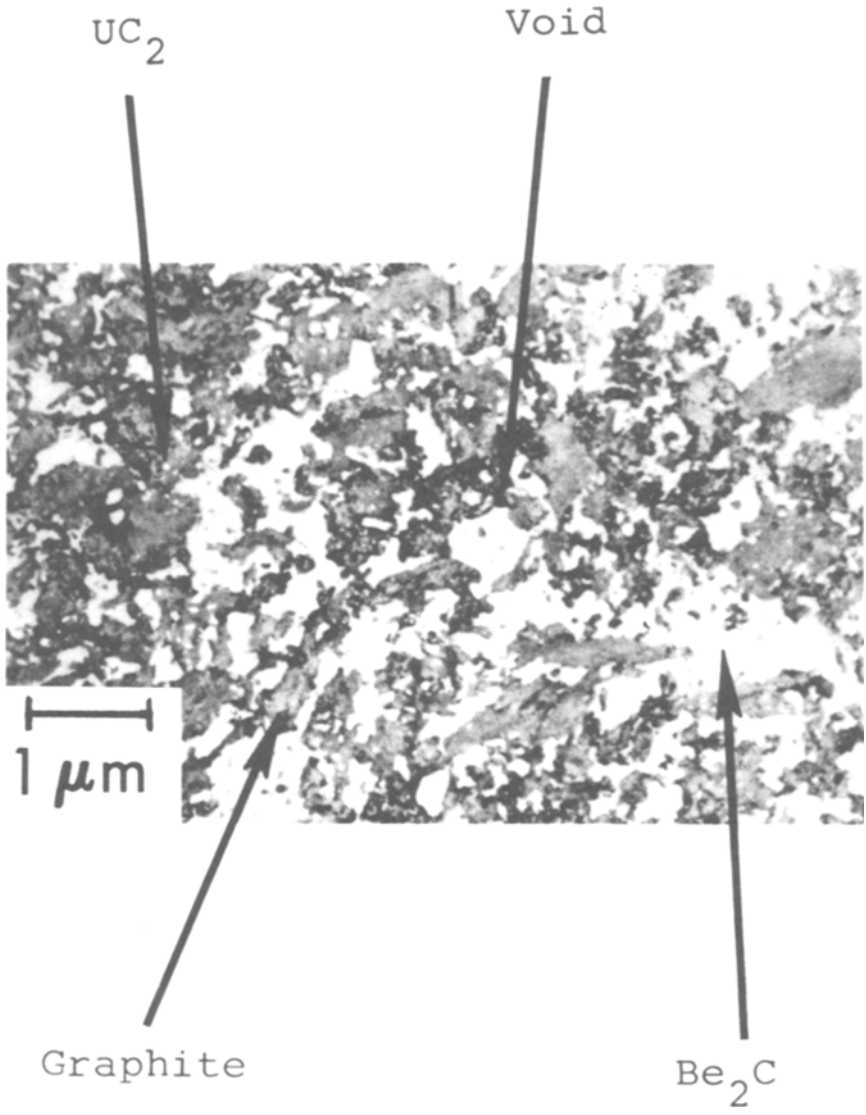

Fig. 3. Photomicrograph showing the microstructure of the Be_2C–Graphite–UC_2 composite fuel material. The white areas are UC_2, light gray is Be_2C, dark gray is graphite, and black is void.

radiography of the composites revealed no detectable UC_2 migration and resulting agglomeration during fabrication. The calorimetry samples were machined from a pressed cylinder. The differential scanning calorimeter samples consisted of small discs (0.61 cm diameter by 0.10 cm thick) and the liquid argon calorimeter samples were cubes (0.64 cm on a side).

2.3. Measurement Procedures

Eight measurements of the low-temperature (298–950 K) specific heat of the fuel material were taken with the differential scanning calorimeter. The temperature measurements were based upon a calibration with a series of pure substances of known melting points, giving a temperature accuracy of 1%. Specific heat was determined with the DSC by recording the difference in power supplied to the sample and a reference material holder as a function of time and temperature. The temperature was scanned at a rate of 10 K per min over a 10 K range centered about the nominal measurement temperature. Three separate temperature scans were required to accurately determine the sample specific heat: (1) a blank scan, in which only empty sample pans were placed on the sample and reference holders to measure the difference in heat capacity, (2) a scan of a sapphire reference sample of known specific heat, placed on the sample side to provide a calibration factor, and (3) a scan using the sample and an empty pan for reference, Data for the run were recorded directly onto the computer, which also controlled the DSC during the measurement.

The liquid argon calorimeter was initially calibrated over a broad range of input power using the electrical calibration system prior to any sample measurements. The electrical calibration allows a final, absolute check of the gas flow measurement system since some error could arise in the measurement of the fluctuating gas flow due to the finite sampling rate. The calibrating energy (Δh_{out}) calculated from the known heat of vaporization of argon and the measured gas flow was found to be within $\pm 2\%$ of the measured electrical heat input (Δh_{in}) over a range of 200–1000 cal (8.37×10^2–4.18×10^3 J). The apparent energy error over this range was expressed as a linear function of Δh_{out}. This allowed correction of the measured heat output to within $\pm 1\%$ of the known heat input. Calibrations were performed frequently during the series of sample measurements to check for any calibration shifts which could arise from equipment malfunction or leaks in the flow system. No shifts were observed to occur.

The measurement procedure for either a calibration or sample measurement consisted of monitoring for 15 min the flow meter background mass flow, monitoring the 5 min peak mass-flow period during heat evolution in the calorimeter, and finally monitoring a 60 min equilibration period. The initial background monitoring period was used to measure the

gas flow due to the heat leak into the dewar. The flow rate during this period was constant to within 0.5%, and the computer recorded the flow at a rate of 15 points per min. The typical background heat leak was approximately 10^{-3} cal · s^{-1} (4.18×10^{-3} J · s^{-1}). The peak period was the interval of maximum heat input to the system either from the sample or the calibration heater. The peak flow rate during this period was over 1000 times greater than the background flow rate. During this period, the computer data rate was increased to 240 points per min. The final monitoring period began when the pressure dropped to a preset level. The computer data rate was then reduced to the initial rate of 15 points per min. The final monitoring period continued for a minimum period of 60 min but at least until the flow rate decreased to within a preset deviation from the initial background flow rate. The barometric pressure in the room was automatically recorded at the beginning and end of each run to correct for changes in the equilibrium temperature of the working fluid. This correction will be discussed in a following section. A period of one hour was usually required after a run to allow the system to return to equilibrium. The computer monitored the background flow and signaled when a constant gas flow rate was achieved. Figure 4 shows a representative plot of

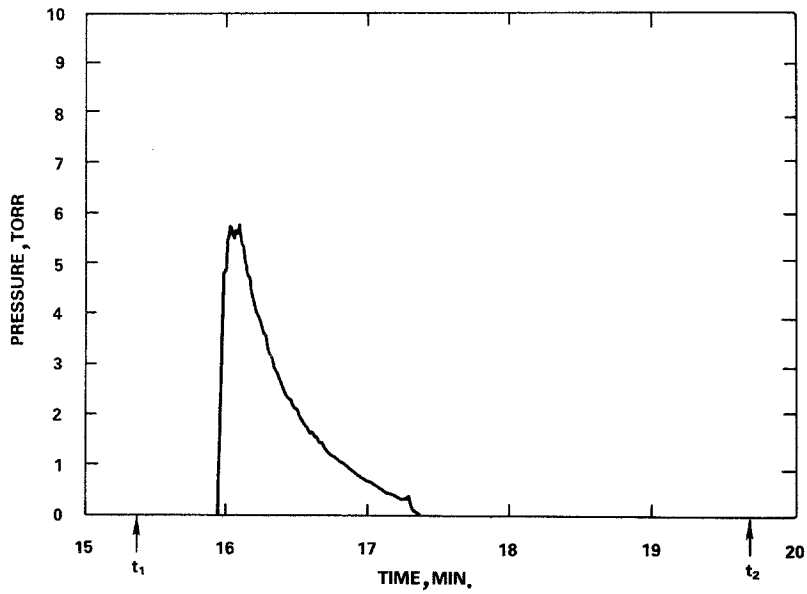

Fig. 4. Measured pressure across the laminar flow unit during peak monitoring period for actual sample heat measurement. t_1 = beginning of peak monitoring period; t_2 = end of peak monitoring period.

Table I. Normal Spectral Emittance of Be_2C–Graphite–UC_2 at 650 nm

T (K)	Emittance
1408	0.81 ± 0.02
1643	0.79 ± 0.05
1786	0.77 ± 0.04
1885	0.75 ± 0.05
1961	0.73 ± 0.04

pressure versus time during the peak monitoring interval for an actual sample measurement. The peak monitoring interval ($t_1 \rightarrow t_2$) is indicated by the arrows.

The sample temperature was determined from the measured brightness temperature and the measured spectral emittance of the material at a wavelength $\lambda = 6.5 \times 10^{-5}$ cm. The spectral emittance of the samples was determined by drilling a cylindrical hole into the sample to approximate a blackbody cavity and measuring the pyrometric temperature in the hole and at the adjacent machined surface. The hole diameter was approximately 0.1 cm and the length/diameter ratio was approximately 5 : 1. This configuration should approximate a true blackbody cavity to within 5% [11]. As a check of the technique, the normal spectral emittance of graphite was measured over the temperature range 1650–2200 K and compared to literature values [12]. The measured graphite emittance (0.78–0.88) were in fair agreement ($< 7\%$) with the literature values, which vary with surface quality by $\approx 7\%$. The emittance of the Be_2C–Graphite–UC_2 material was measured over the same temperature range for two separate samples. The emittances and the corresponding error limits determined from the differences seen between the two samples are listed in Table I.

3. CALCULATIONS AND RESULTS

3.1. Temperature Measurement

The true blackbody temperature T (in K) of the samples was calculated using an equation derived from Wien's formula,

$$T = (\lambda \cdot \ln(\epsilon)/1.4388 + 1/T_s)^{-1} \tag{1}$$

where λ is the pyrometer wavelength (6.5×10^{-5} cm), ϵ is the normal spectral emittance, and T_s is the brightness temperature. The emittance was represented by a linear regression fit to the data in Table I. In addition, all

temperature measurements were adjusted for transmission and reflectance losses through the quartz sighting window.

3.2. Specific Heat and Enthalpy

The specific heat data obtained with the DSC were computed by numerical integration of the differential power data recorded by the computer. The low-temperature enthalpy was calculated by smoothing the specific heat data obtained with the DSC and then integrating the smoothed data with respect to temperature. The DSC data are listed in Table II.

The sample enthalpy data obtained with the liquid argon calorimeter were computed from the measured pressure drop across the laminar flow unit. The mass flow was calculated from the measured pressure values using the calibration function for the laminar flow unit and the density of the argon gas at the reference bath temperature. The heat flow ($\dot{Q}$) was calculated from the measured mass flow using the heat of vaporization of the liquid argon at the measured equilibrium pressure. The heat flow was corrected for heat leakage rate into the dewar (l) determined during the initial background monitoring period. The total heat output during the peak monitoring period ($t_1 \rightarrow t_2$) was determined by direct numerical integration using the trapezoidal rule. In the final background period, the rate of heat transfer was assumed to obey Newtonian cooling and was represented as a function of time t by the equation

$$\dot{Q} - l = Ae^{-Bt} \qquad (t > t_2) \tag{2}$$

The measured background flow was fit using a linear regression routine to determine the coefficients A and B. Although the background flow rate was

Table II. Experimentally Measured Specific Heat Data of Be_2C–Graphite–UC_2 Obtained with the DSC

T (K)	C_p (cal · g^{-1} · K^{-1})
298	0.205
400	0.273
500	0.324
600	0.358
700	0.384
790	0.405
900	0.427
950	0.436

approximately 1000 times smaller than the flow rate in the peak period, approximately 10% of the total energy was released during the final background period. The total heat output was given by the equation

$$\Delta h_{\text{out}} = \int_{t_1}^{t_2} (\dot{Q} - l)\, dt + \int_{t_2}^{\infty} A e^{-Bt}\, dt \tag{3}$$

The enthalpy was computed using this result and the mass of the sample and was referenced to the temperature of the liquid argon bath (≈ 85 K). The resulting equation is given by

$$H_T - H_{85} = \Delta h_{\text{out}}/m \tag{4}$$

where m is the mass of the sample. The enthalpy was referenced to room temperature by measuring $\Delta h_{\text{out}}/m$ for a room temperature (298.15 K) sample and subtracting this result from values obtained at higher temperatures as follows:

$$H_T - H_{298} = (H_T - H_{85}) - (H_{298} - H_{85}) \tag{5}$$

This value was corrected for systematic system errors using the correction factor determined from the electrical calibration ($< 1\%$). Corrections were also made for the volume of liquid argon vaporized in the dewar as a result of heat input ($< 0.5\%$) and for changes in the equilibrium pressure in the dewar ($< 1\%$).

Heat loss occurred from the samples during the period of fall between the sample chamber and the liquid argon surface. The loss occurred due to radiation by the sample and convective heat transfer to the argon gas. The radiation loss was calculated using the Stefan–Boltzmann law and the measured specific heat of the sample [13]. The convective loss was calculated using an engineering equation based on the heat transfer between spheres and air [13, 14]. The convective loss equation was modified for loss to the argon gas using known properties of argon gas [15]. The estimated heat loss from the sample during the fall period never exceeded 3% of the measured enthalpy.

The enthalpy data obtained from the DSC and the liquid argon calorimeter were combined and fit with a spline routine over the entire temperature range 298–1980 K [16]. The measured enthalpies and the spline fit are shown graphically in Fig. 5, and the values are tabulated in Table III. The fit to the DSC data was excellent, with all deviations from the curve less than 0.3%. The maximum deviation of the liquid argon calorimeter data from the curve was 3.5%. These larger deviations were

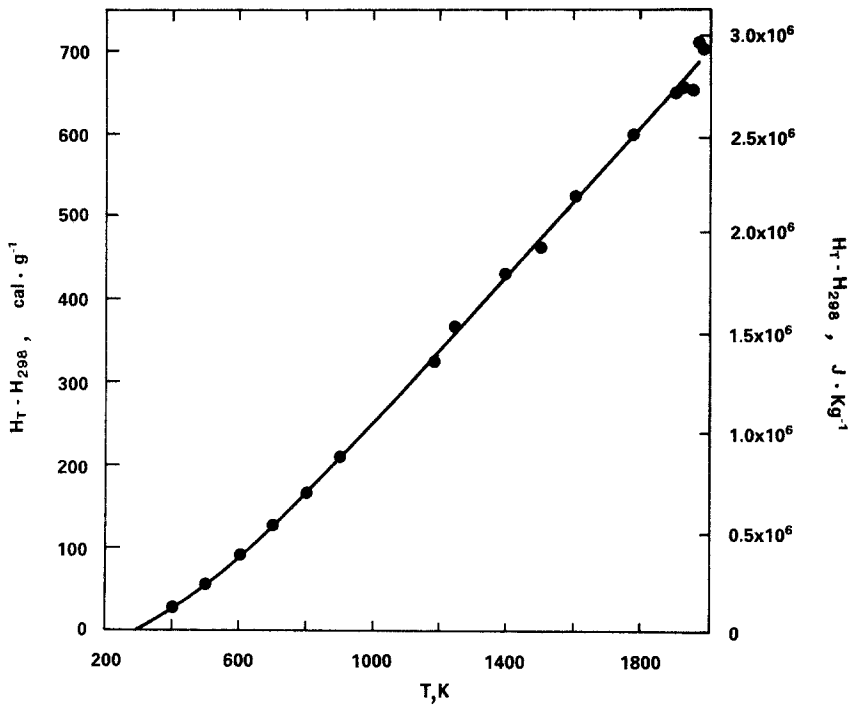

Fig. 5. Enthalpy, $H_T - H_{298}$, of the Be_2C–Graphite–UC_2 fuel material. The solid curve represents the spline fit to the data. All data for $T \leqslant 900$ K were obtained with the DSC. Data for $T \geqslant 1185$ K were obtained with the liquid argon vaporization calorimeter.

partially due to uncertainty in the measured temperature and possible temperature gradients in the sample.

The specific heat was given by the first derivative of the spline fit and is shown in Fig. 6 (tabulated values are listed in Table III). As one check of the sensitivity of the calculated specific heat to the functional representation of the enthalpy, the enthalpy was fit with an alternate equation of the form

$$H = a + bT + cT^2 + d/T \tag{6}$$

a representation often used to fit high temperature enthalpy data [17]. The specific heat determined from this function agreed with the spline fit specific heat within 1.5% for $T \geqslant 700$ K, while the error below this temperature was $\approx 5\%$. (The values of the coefficients used in Eq. (6) are listed in Table III.) This analysis suggests that the specific heat is insensitive

Table III. Experimentally Determined Data for the Enthalpy of Be_2C–Graphite–UC_2 and Spline-Fit Generated Values for Enthalpy and Specific Heat

	Experimental[a,b]	Spline fit[c,d]	% Difference	(From Spline Fit)
T (K)	$H_T - H_{298}$ $(\text{cal} \cdot \text{g}^{-1})$	$H_T - H_{298}$ $(\text{cal} \cdot \text{g}^{-1})$	$\frac{\text{Exp.-fit}}{\text{Exp.}} \times 100$	C_p $(\text{cal} \cdot \text{g}^{-1} \cdot K^{-1})$
298	0.0	0.0	—	0.212
400	24.2	24.3	− 0.4	0.272
500	54.1	53.9	0.4	0.321
600	88.3	88.1	0.2	0.360
700	125.6	125.7	− 0.1	0.389
800	165.2	165.8	− 0.4	0.407
900	206.8	207.2	− 0.2	0.420
1185	323.4	330.8	− 2.2	0.444
1241	365.8	355.7	2.8	0.447
1390	428.9	422.5	1.5	0.451
1498	461.7	471.1	− 2.0	0.451
1599	523.0	516.7	1.2	0.452
1605	520.4	519.4	0.2	0.452
1778	598.6	597.8	0.1	0.456
1899	647.9	653.2	− 0.8	0.460
1922	656.9	663.8	− 1.0	0.460
1947	652.6	675.4	− 3.4	0.461
1968	708.0	685.1	3.3	0.462
1980	700.4	690.7	1.4	0.463

[a] $1.0\ \text{cal} \cdot \text{g}^{-1} = 4.184 \times 10^3\ \text{J} \cdot \text{kg}^{-1}$.

[b] Data for $T \leqslant 900$ K was obtained by curve fitting the specific heat data obtained on the DSC and then integrating over temperature.

[c] Spline equation: temperature range 298–784 K

$$H_T - H_{298} = 0.2047\,(T - 298) + 3.448 \times 10^{-4}\,(T - 298)^2 - 1.890 \times 10^{-7}\,(T - 298)^3$$

temperature range 784–1420 K

$$H_T - H_{298} = 159.2 + 0.4059\,(T - 784) + 6.915 \times 10^{-5}\,(T - 784)^2 - 3.625 \times 10^{-8}\,(T - 784)^3$$

temperature range 1420–1980 K

$$H_T - H_{298} = 436.0 + 0.4499\,(T - 1420) + 5.940 \times 10^{-18}\,(t - 1420)^2 + 1.526 \times 10^{-8}\,(T - 1420)^3$$

[d] Fitting parameters to alternate equation of form:

$$H = a + bT + cT^2 + d/T \quad \text{(where } H \text{ is in cal} \cdot \text{g}^{-1}\text{, and } T \text{ is in K)}$$

$$a = -215.5 \qquad b = 0.4312 \qquad c = 1.0312 \times 10^{-5} \qquad d = 2.5024 \times 10^4$$

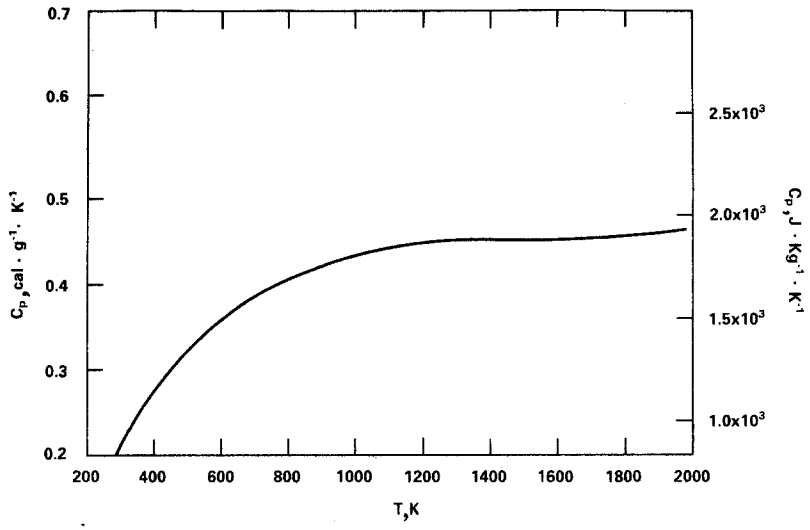

Fig. 6. Specific heat of the Be_2C–Graphite–UC_2 composite fuel material obtained from the first derivative of the spline fit. Tabulated values are listed in Table III.

to the functional representation of the enthalpy data in this experiment. Another possible source of error in the calculated specific heat was the uncertainty in the sample emittance. A sensitivity analysis with respect to emittance was performed, and the maximum resulting error in the specific heat was 1.5%. The estimated total error in the calculated specific heat is $< 5\%$.

3.3. Discussion

Calculation of the enthalpy and specific heat of the Be_2C–Graphite–UC_2 composite requires data for the specific heat or enthalpy of the three primary materials (Be_2C, graphite, UC_2). Previous work has shown that the additivity of heat capacity holds for these types of materials [3]. However, only limited experimental values exist for the specific heat and enthalpy of Be_2C and UC_2 [5, 18–20]. The Be_2C has only been measured in an impure state at low temperatures ($T < 1470$ K) and the specific heat extrapolated to higher temperatures [19]. Uncertainty also exists in the data for UC_2, which can be affected by UC precipitation at higher temperatures ($T > 1000$ K) [18]. Literature values of the specific heat of the primary materials are listed in Table IV over the temperature range 298–1980 K. The data for each material were fit with polynomial functions of tempera-

Table IV. Literature Values of Specific Heat (cal · g^{-1} · K^{-1}) for Primary Components of Be_2C–Graphite–UC_2

T (K)	Be_2C[a]	Graphite[b]	UC_2[c]
298	0.343	0.169	0.056
400	0.378	0.238	0.062
600	0.448	0.336	0.069
800	0.517	0.393	0.073
1000	0.585	0.428	0.076
1200	0.652	0.453	0.081
1400	0.718	0.470	0.088
1600	0.783	0.484	0.098
1800	0.847	0.494	0.110
2000	0.910	0.503	0.123

[a] From ref. [19].
[b] From ref. [6].
[c] From ref. [20].

ture (Table V) and integrated to obtain the corresponding enthalpy (Table VI).

Table VII lists the enthalpy and specific heat of the composite material calculated from the literature values in Tables IV and VI along with the values obtained by the spline fit to the experimental data. This table shows that the experimental enthalpy deviates over 7% from the enthalpy calculated using the literature values, while the experimental specific heat deviates by more than 22% at higher temperatures. The differences between the literature and experimental specific heat values are significantly greater than the experimental error limit of 5% and indicate a deviation in the temperature dependent specific heat of one or more of the components from the reported values. Although some uncertainty exists in the value of the specific heat for the graphite component, a calculation of the composite specific heat using two separate representations of the graphite contribution changes the composite specific heat by less than 3% [6, 21]. Uncertainty in the specific heat of UC_2 is not a significant source of error either since the UC_2 contributes only $\approx 3\%$ to the total composite specific heat. Therefore, the most probable source of error in the "calculated" composite specific heat is the literature value for the specific heat of the Be_2C component.

The specific heat of Be_2C is estimated from the experimental specific heat data of the composite using the literature values for the specific heat contributions for the other two components and the known weight percent of Be_2C. The result of this calculation is shown in Fig. 7. A third-order

Table V. Polynomial Coefficients for Curve Fit to Literature Values of Specific Heat of the Primary Components of Be_2C–Graphite–UC_2[a]

$$C_p = A + BT + CT^2 + DT^3 + ET^4$$

	Graphite[b]			Be_2C[c]	UC_2[d]
	(298–813 K)	(813–1863 K)	(1863–2073 K)	(298–2073 K)	(298–2073 K)
A	-8.71×10^{-2}	-6.00×10^{-2}	0.351	0.235	2.31×10^{-2}
B	8.99×10^{-4}	1.09×10^{-3}	1.12×10^{-4}	3.62×10^{-4}	1.61×10^{-4}
C	1.76×10^{-7}	-9.17×10^{-7}	-1.81×10^{-8}	-1.22×10^{-8}	-2.04×10^{-7}
D	-1.27×10^{-9}	3.77×10^{-10}	0	0	1.17×10^{-10}
E	7.27×10^{-13}	-6.06×10^{-14}	0	0	-2.13×10^{-14}

[a] C_p in cal · g^{-1} · K^{-1}, T in K.
[b] From ref. [6].
[c] From ref. [19].
[d] From ref. [20].

Table VI. Enthalpy (in cal · g^{-1}) for Primary Components of Be_2C–Graphite–UC_2 Computed from Literature Values by Integration of Curve Fit Polynomials Listed in Table V

T (K)	Be_2C	Graphite	UC_2
298	0.0	0.0	0.0
400	36.7	20.8	6.0
600	119.3	79.0	19.2
800	215.7	152.4	33.3
1000	325.9	234.8	48.1
1200	449.5	323.0	63.7
1400	586.4	415.4	80.5
1600	736.5	510.8	99.1
1800	899.4	608.6	119.9
2000	1075.0	708.3	143.4

polynomial curve fit is shown by the solid line through the data points, which approaches a value of approximately 0.56 cal · g^{-1} · K^{-1} (2.3×10^3 J · kg^{-1} · K^{-1}) for $T > 1000$ K. The calculated specific heat from ref. [19] (dashed line) is also shown for comparison. The uncertainty in this derived specific heat is $\approx 10\%$ based upon assumed uncertainties of 5% in the

Table VII. Comparison of Experimentally Determined Enthalpy and Specific Heat of Be_2C–Graphite–UC_2 Computed from Primary Components Reported in the Literature

T (K)	$H_T - H_{298}$ (cal · g^{-1})			C_p (cal · g^{-1} · K^{-1})		
	Literature	Exp.[a]	% Diff.[b]	Literature	Exp.[c]	% Diff.
298	0.0	0.0	—	0.218	0.212	− 2.8
400	24.6	24.3	− 1.2	0.264	0.272	3.0
600	85.0	88.2	3.8	0.336	0.360	7.1
800	157.6	165.6	5.1	0.389	0.407	4.6
1000	239.8	249.6	4.1	0.432	0.431	− 0.2
1200	330.0	337.4	2.2	0.470	0.445	− 5.3
1400	427.4	427.2	− 0.1	0.504	0.451	− 10.5
1600	531.6	517.3	− 2.7	0.537	0.452	− 15.8
1800	642.2	608.0	− 5.3	0.569	0.456	− 19.9
2000	759.1	700.0	− 7.8	0.600	0.464	− 22.7

[a] From spline fit to experimental data.
[b] % Diff. = 100 × (exp. − lit.)/lit.
[c] From differentiation of spline fit.

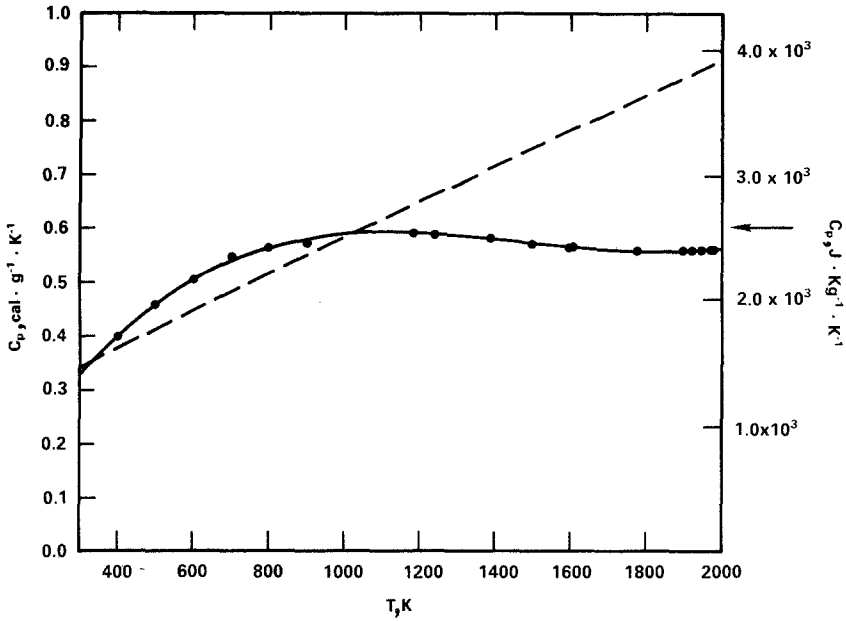

Fig. 7. Specific heat of Be_2C, solid circles, obtained from the measured specific heat of the composite fuel material and the "calculated" specific heat contributions from the literature values of graphite and UC_2. The solid line through the data points is a third-order polynomial curve fit given by

$$C_p = a + bT + cT^2 + dT^3$$

where C_p is in cal · g^{-1} · K^{-1}, T in K, and $a = 2.054 \times 10^{-2}$, $b = 1.292 \times 10^{-3}$, $c = -9.348 \times 10^{-7}$, and $d = 2.124 \times 10^{-10}$. The dashed line is the calculated value given in ref. [19]. The arrow at the right is the classical limit given by the law of Dulong and Petit.

specific heat of each component and the experimental values for the composite. The arrow at the right of the figure shows the classical upper limit of the specific heat (0.61 cal · g^{-1} · K^{-1} [2.34×10^3 J · kg^{-1} · K^{-1}]) calculated from the law of Dulong and Petit and the law of atomic fractions [5].

The conclusions drawn from this study for the composite fuel Be_2C–Graphite–UC_2 are that the addition of Be_2C results in a significant increase in enthalpy over previous fuels studied but that the high temperature specific heat is less ($\approx$23% at 2000 K) than expected from data reported in the literature. Use of the specific heat data for Be_2C calculated from the measured composite specific heat should improve future estimates of the thermodynamic properties of other Be_2C composites.

ACKNOWLEDGMENTS

This work was performed at Sandia National Laboratories and supported by the U.S. Department of Energy under contract DE-AC04-76DP00789. The author expresses his appreciation to R. H. Marion for providing the fuel samples and to H. P. Stephens for consultation on the liquid argon calorimeter. The author also thanks T. V. Tormey for performing the actual calorimetric measurements.

REFERENCES

1. D. J. Sasmor, J. A. Reuscher, P. S. Pickard, J. B. Rivard, J. S. Philbin, and R. L. Coats, *Trans. Am. Nucl. Soc.* **19**:129 (1974).
2. D. J. Sasmor, P. S. Pickard, and J. B. Holt, *Trans. Am. Nucl. Soc.* **27**:246 (1977).
3. H. P. Stephens, in *Proceedings of the Seventh Symposium on Thermophysical Properties* (ASME, New York, 1977), p. 351.
4. R. H. Marion and W. A. Muenzer, *Trans. Am. Nucl. Soc.* **28**:204 (1978).
5. Y. S. Touloukian and E. H. Buyco, *Specific Heat: Nonmetallic Solids*, (IFI/Plenum, New York, 1970).
6. A. T. D. Butland and R. J. Maddison, *J. Nucl. Mater.* **49**:45 (1973).
7. H. P. Stephens, *High Temp. Sci.* **6**:156 (1974).
8. H. P. Stephens, *High Temp. Sci.* **10**:95 (1978).
9. R. O. Williams, *Rev. Sci. Instrum.* **34**:639 (1963).
10. W. P. Gilbreath and D. E. Wilson, *Rev. Sci. Instrum.* **41**:969 (1970).
11. R. E. Bedford and C. K. Ma, *J. Opt. Soc. Am.* **64**:339 (1974).
12. Y. S. Touloukian and D. P. DeWitt, *Thermal Radiative Properties: Non-Metallic Solids* (IFI/Plenum, New York, 1972).
13. D. W. Bonnell, Ph.D. Thesis, Rice University, Houston, Tex. (1972), p. 60.
14. W. H. McAdams, *Heat Transmission* (McGraw-Hill, New York, 1954), p. 265.
15. J. Hilsenrath et al., *Tables of Thermodynamic and Transport Properties of Air, Argon, CO_2, CO, H_2, N_2, O_2, and Steam* (Pergamon Press, Elsmford, N.Y., 1960).
16. J. F. Lathrop, D. L. Crawford, and R. J. Hanson, *DATFIT—User's Manual, An Interactive Constrained Least Squares Data Fitting Program*, Sandia Labs. Report SAND 80–8204 (Mar. 1980). Available from: National Technical Information Service (NTIS). U.S. Dept. of Commerce, 5285 Port Royal Road, Springfield, VA 22161.
17. C. G. Maier and K. K. Kelley, *J. Am. Chem. Soc.* **54**:3243 (1932).
18. E. K. Storms, *The Refractory Carbides* (Academic Press, New York, 1967).
19. J. Neely, C. Teeter, and J. Trice, *J. Am. Ceram. Soc.* **33**:363 (1950).
20. L. S. Levinson, *J. Chem. Phys.* **38**:2105 (1963).
21. R. H. Marion, Sandia National Laboratories, personal communication.